

# A Natural Scotogenic Model for Neutrino Mass & Dark Matter

Amine Ahriche,<sup>1,2,3,\*</sup> Adil Jueid,<sup>4,†</sup> and Salah Nasri<sup>5,2,‡</sup>

<sup>1</sup>*Department of Applied Physics and Astronomy, University of Sharjah, P.O. Box 27272 Sharjah, UAE.*

<sup>2</sup>*The Abdus Salam International Centre for Theoretical Physics, Strada Costiera 11, I-34014, Trieste, Italy.*

<sup>3</sup>*Laboratoire de Physique des Particules et Physique Statistique,*

*Ecole Normale Supérieure, BP 92 Vieux Kouba, DZ-16050 Algiers, Algeria.*

<sup>4</sup>*Department of Physics, Konkuk University, Seoul 05029, Republic of Korea.*

<sup>5</sup>*Department of physics, United Arab Emirates University, Al-Ain, UAE.*

In this letter, we propose an extension of the scotogenic model where singlet Majorana particle can be dark matter (DM) without the need of a highly suppressed scalar coupling of the order  $O(10^{-10})$ . For that, the SM is extended with three singlet Majorana fermions, an inert scalar doublet, and two (a complex and a real) singlet scalars, with a global  $Z_4$  symmetry that is spontaneously broken into  $Z_2$  at a scale higher than the electroweak one by the vev of the complex singlet scalar. In this setup, the smallness of neutrino mass is achieved via the cancellation between three diagrams a la scotogenic, a DM candidate that is viable for a large mass range; and the phenomenology is richer than the minimal scotogenic model.

## I. INTRODUCTION

Various astrophysical and cosmological observations indicate the existence of a weakly or super-weakly interacting particle and which its density constitutes about 85% of matter in the universe. On the other hand, the data from neutrino oscillations imply that neutrinos have a tiny mass, more than six order of magnitudes lighter than the electron. Hence, understanding the origin of neutrino mass and the nature of dark matter (DM) are among the strongest motivations for going beyond the standard model (SM) of particle physics. In particular, one hope to address these two puzzles within the same framework.

A natural explanation for the smallness neutrino mass,  $m_\nu$ , is via the seesaw mechanism where the hierarchy between the electron and neutrino masses is due to the hierarchy between the electroweak (EW) scale and the singlet Majorana fermion, a new degree of freedom that is added to the SM. However, for Yukawa couplings of order unity, the Majorana fermion mass is many order of magnitude larger than the EW scale, making it impossible to probe at the current and near future high energy colliders. In addition, within this scenario there is no DM candidate as the lightest Majorana fermion is unstable. An attractive alternative is the radiative neutrino mass mechanism in which neutrinos are massless at tree level and acquire a naturally small Majorana mass term at loop level [1–10] (see [11, 12] for a review). In such models neutrino masses are calculable and their smallness follows from Loop suppression factors and products of the Yukawa couplings. Consequently, the new degrees of freedom that couple to the SM particles can be of the order of the electroweak scale, and hence will potentially be accessible at high energy colliders. Furthermore, many radiative neutrino mass models naturally provide dark matter candidate which itself plays a central role in generating small mass for neutrino.

The simplest realization of this neutrino-mass generation mechanism is provided by the scotogenic model [5], which is a minimal extension of the SM by an inert scalar doublet and three singlet Majorana fermions. In this framework, the neutrinos gets their small masses at the one-loop level. Besides, the model

---

\*Electronic address: [ahriche@sharjah.ac.ae](mailto:ahriche@sharjah.ac.ae)

†Electronic address: [adil.hep@gmail.com](mailto:adil.hep@gmail.com)

‡Electronic address: [snasri@uaeu.ac.ae](mailto:snasri@uaeu.ac.ae)

allows for two possible candidates for DM: the lightest Majorana fermion, or the lightest neutral scalar in the inert dark doublet <sup>1</sup>, which is highly constrained by the DM direct detection experiments.

However, in order to generate tiny neutrino mass in the minimal scotogenic model, one needs either to make the Yukawa coupling in the new interactions extremely small, or to enforce a mass-degeneracy between the  $CP$ -odd and the  $CP$ -even scalars. Moreover, all the new Yukawa couplings are renormalized multiplicatively [24], and hence small new Yukawa couplings values are stable against radiative corrections and will remain small along the renormalization group flow. Similar feature can be noticed for the coupling  $\lambda_5$ , contrary to the couplings  $\lambda_3$  and  $\lambda_4$ , if it is chosen to be zero at the electroweak scale, it remains so at higher energy scale.

In the case of scalar DM candidate, the right amount of the relic density can be achieved only by considering the co-annihilation effect [25]<sup>2</sup>, or/and via the assistance of the lightest Majorana fermion decay [26]. In addition, to avoid the constraints on the DM-Nucleus scattering cross section, we must have a suppression on the Higgs-DM coupling  $\lambda_L = \lambda_3 + \lambda_4 \pm \lambda_5$ . However, the coupling  $\lambda_5$  does not need to be suppressed in this case, and therefore the mass degeneracy between the  $CP$ -even and  $CP$ -odd is not sharp. Consequently, the required small values of the new Yukawa couplings make this case less interesting for both collider and LFV experiments. This makes the scalar DM case not the most attractive option for the scotogenic model.

On the other hand, the lightest singlet Majorana fermion is an interesting alternative since constraints from direct detection experiments do not significantly affect the model parameters due to the fact that spin-independent cross section  $\sigma_{SI}$  is induced at the one-loop order [27]. However, in this case, the small Yukawa couplings imply that (i) the relic density is above the Planck measurement since the annihilation cross section becomes extremely small, (ii) the lepton flavor violating (LFV) decays occur with extremely small branching ratios (many orders of magnitude smaller than the experimental bounds), and hence it is almost hopeless for the model to be probed at experiments searching for such processes, (iii) the DM-Nucleus scattering cross section is below the neutrino floor for most regions of the parameter space, making it impossible to detect it in DM direct detection experiments. Therefore, for Majorana DM, the only viable scenario is to enforce a mass-degeneracy between the  $CP$ -odd and the  $CP$ -even scalars. Thus, it is the aim of this paper to provide a natural explanation for the smallness of neutrino mass without imposing highly suppressed values of  $\lambda_5$  and, therefore, addressing the problems of DM and LFV with non-suppressed new Yukawa couplings which could be interesting at colliders. To do so, we extend the scotogenic model with two singlet scalar fields; one real and one complex; and transform under a global  $Z_4$  symmetry that is spontaneously broken by the complex singlet scalar vev at an energy scale much higher than the EW scale. Due to this high scale, the mixing of the complex singlet scalar with neutral inert can be safely neglected, and therefore one can study the effective interactions model after the  $Z_4$  breaking. This is a minimal extension of the model while retaining the concept of the scotogenic mechanism, without suffering from the aforementioned issues for most of the space parameters. Another extension of the minimal scotogenic model by a real scalar field that mixes with the  $CP$ -even field without imposing any discrete symmetry larger than  $Z_2$  [28]. In this case, the new singlet modifies both the phenomenology of neutrino masses, relaxes the constraints from the scalar DM relic density, and opens up a large portion of the parameter space than the original model.

The paper is organized as follows. In section II, we present the model, and its parameters. In section III, we derive the expression of the neutrino mass within the model. Section IV is devoted to the theoretical and the experimental constraints on the model parameter space. Then, in section V we study the DM phenomenology of the model assuming the DM candidate to be a Majorana fermion. In section VI, we briefly discuss the collider signatures of this model in hadronic colliders pointing out the main differences between this model and the minimal scotogenic one. We conclude in section VII.

---

<sup>1</sup> The phenomenology of the scotogenic model has been extensively studied in the literature [13–23].

<sup>2</sup> Here, the scalar DM in the minimal scotogenic model is potentially indistinguishable from inert Higgs doublet model at high energy colliders and DM direct detection experiments.

## II. THE MODEL

We extend the SM by an inert Higgs doublet denoted by  $\Phi$ , three singlet Majorana fermions  $N_i$ , a real singlet scalars  $S$ ; and a complex scalar  $\chi$ . Their quantum numbers under the  $SU(3)_c \otimes SU(2)_L \otimes U(1)_Y$  group are depicted below

$$\Phi : (1, 2, 1), \quad N_i : (1, 1, 0), \quad S : (1, 1, 0), \quad \chi : (1, 1, 0). \quad (1)$$

The Lagrangian that involves the Majorana fermions can be written as

$$\mathcal{L} \supset h_{\alpha i} \bar{L}_\alpha \epsilon \Phi N_i + \frac{1}{2} M_i \bar{N}_i^C N_i + h.c., \quad (2)$$

where  $L_\alpha$  are the left-handed lepton doublets, and  $\epsilon = i\sigma_2$  is an anti-symmetric tensor.

In this setup, the Lagrangian is invariant under a global  $Z_4$  symmetry, that is spontaneously broken by the vacuum expectation value of the complex scalar  $\langle \chi \rangle \neq 0$  at an energy scale much higher than the electroweak scale<sup>3</sup>, and below this scale the Lagrangian has a residual to  $Z_2$  symmetry. The charge assignment of the fields under both  $Z_4$  and  $Z_2$  are given in Table I.

|       | $\chi$ | $S$  | $N_i$ | $\Phi$ | $L_\alpha$ | $\ell_{R\alpha}$ | $X_{SM}$ |
|-------|--------|------|-------|--------|------------|------------------|----------|
| $Z_4$ | $i$    | $-1$ | $-1$  | $-i$   | $i$        | $i$              | $+1$     |
| $Z_2$ |        | $-1$ | $-1$  | $-1$   | $+1$       | $+1$             | $+1$     |

**TABLE I:** The field charges under the symmetries  $Z_4$  at energy scale  $\gg \langle H \rangle$ ; and  $Z_2$  around the electroweak scale (where  $\chi$  decouples), where  $X_{SM}$  denotes all SM fields except the left-handed leptons  $L_\alpha$  and the charged right-handed leptons  $\ell_{R\alpha}$ .

The most general  $Z_2$ -symmetric,  $CP$ -conserving, renormalizable, and gauge invariant potential reads<sup>4</sup>

$$\begin{aligned} V(H, \Phi, S, \chi) \supset & -\mu_1^2 |H|^2 + \mu_2^2 |\Phi|^2 + \frac{\mu_S^2}{2} S^2 + \frac{\lambda_1}{6} |H|^4 + \frac{\lambda_2}{6} |\Phi|^4 + \frac{\lambda_S}{24} S^4 + \lambda_3 |H|^2 |\Phi|^2 \\ & + \lambda_4 |H^\dagger \Phi|^2 + \frac{\omega_1}{2} |H|^2 S^2 + \frac{\omega_2}{2} |\Phi|^2 S^2 + \left\{ \zeta S H^\dagger \Phi + h.c. \right\}, \end{aligned} \quad (3)$$

with  $H$ , and  $\Phi$  can be parameterized as follows

$$H = \begin{pmatrix} G^+ \\ \frac{1}{\sqrt{2}}(v + h + iG^0) \end{pmatrix}, \quad \Phi = \begin{pmatrix} H^+ \\ \frac{1}{\sqrt{2}}(H^0 + iA^0) \end{pmatrix}. \quad (4)$$

The terms of the Lagrangian in (2) and (3) are invariant under a global  $Z_2$  symmetry according to the charges given in Table I. One has to mention that the assigned charges according to  $Z_4$  forbids the existence of the term  $(H^\dagger \Phi)^2$  in the Lagrangian before or after the  $Z_4$  breaking.

After the electroweak symmetry breaking (EWSB), we are left with three  $CP$ -even scalars ( $h, H_1^0, H_2^0$ ), one  $CP$ -odd scalar  $A^0$  and a pair of charged scalars  $H^\pm$ . Their tree-level masses are given by:

$$m_{H^\pm}^2 = \mu_2^2 + \frac{\lambda_3}{2} v^2, \quad m_{A^0}^2 = m_{H^\pm}^2 + \frac{\lambda_4}{2} v^2, \quad m_{H_1^0, H_2^0}^2 = \frac{1}{2} \left\{ m_S^2 + m_{A^0}^2 \mp \sqrt{(m_S^2 - m_{A^0}^2)^2 + 4\zeta^2 v^2} \right\} \quad (5)$$

<sup>3</sup> In this case the mixing of the  $CP$ -even part of the neutral component of the Higgs doublet with the real part of  $\chi$  will be very small, and this will not affect DM relic density or the neutrino mass.

<sup>4</sup> Here, the Lagrangian term  $\{\zeta S H^\dagger \Phi + h.c.\}$  in (3) emerges from the term  $\{\kappa \chi S H^\dagger \Phi + h.c.\}$  after the  $Z_4$  symmetry breaking, i.e.,  $\zeta = \kappa < \chi >$ .

with  $m_S^2 = \mu_S^2 + \frac{\omega_1}{2}v^2$ , and  $\alpha$  is the angle that diagonalises the  $CP$ -even mass matrix, i.e.

$$\begin{pmatrix} H_1^0 \\ H_2^0 \end{pmatrix} = \begin{pmatrix} c_\alpha & s_\alpha \\ -s_\alpha & c_\alpha \end{pmatrix} \begin{pmatrix} H^0 \\ S \end{pmatrix}, \quad t_{2\alpha} = \frac{4\sqrt{(m_{H_2^0}^2 - m_{A^0}^2)(m_{A^0}^2 - m_{H_1^0}^2)}}{m_{H_1^0}^2 + m_{H_2^0}^2 - 2m_{A^0}^2}, \quad (6)$$

with  $c_\alpha \equiv \cos \alpha$ ,  $s_\alpha \equiv \sin \alpha$ , and  $t_{2\alpha} = \tan 2\alpha$ . Equation 5 implies the following mass ordering

$$m_{H_2^0} \geq m_{A^0} \geq m_{H_1^0}$$

Therefore the only possible scalar DM candidate is the light  $CP$ -even scalar  $H_1^0$ . Besides, the decoupling limit could be achieved only if the parameter  $m_S^2$  is very large with respect to  $|\xi|v$ . The model involves thirty-one additional parameters where two of them  $\mu_1^2$  and  $v$  are absorbed into the definition of the  $W$ -boson and the SM Higgs boson masses. The independent parameters are chosen as follows:

$$\left\{ M_i, m_{A^0}, m_{H^\pm}, m_{H_1^0}, m_{H_2^0}, h_{\alpha i}, \lambda_2, \lambda_3, \omega_1, \omega_2 \right\}. \quad (7)$$

### III. NEUTRINO MASS

The neutrino mass could be generated via the three one-loop diagrams shown in Fig. 1.

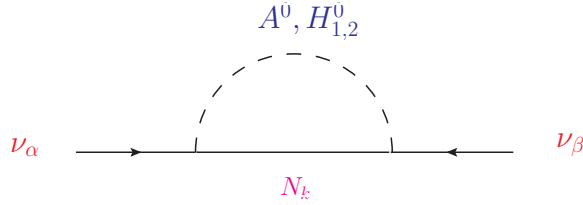


FIG. 1: Feynman diagrams responsible for neutrino mass.

The neutrino mass matrix elements can be written as

$$m_{\alpha\beta}^{(\nu)} = \sum_k \frac{h_{\alpha k} h_{\beta k} M_k}{16\pi^2} \left\{ c_\alpha^2 \mathcal{F}\left(\frac{m_{H_1^0}^2}{M_k^2}\right) + s_\alpha^2 \mathcal{F}\left(\frac{m_{H_2^0}^2}{M_k^2}\right) - \mathcal{F}\left(\frac{m_{A^0}^2}{M_k^2}\right) \right\}, \quad (8)$$

where  $\mathcal{F}(x) = x \log(x)/(x-1)$ . Then, according to the Casas-Ibarra parameterization, the Yukawa couplings would have the generic form [29]

$$h = D_{\sqrt{\Lambda^{-1}}} R D_{\sqrt{m_\nu}} U_\nu^T, \quad (9)$$

with  $D_{\sqrt{\Lambda^{-1}}} = \text{diag} \left\{ \Lambda_1^{-1/2}, \Lambda_2^{-1/2}, \Lambda_3^{-1/2} \right\}$ ,  $D_{\sqrt{m_\nu}} = \text{diag} \left\{ m_1^{1/2}, m_2^{1/2}, m_3^{1/2} \right\}$ ,  $R$  is an arbitrary  $3 \times 3$  orthogonal matrix,  $m_i$  are the neutrino mass eigenstates and  $U_\nu$  is the Pontecorvo-Maki-Nakawaga-Sakata (PMNS) mixing matrix; and

$$\Lambda_k = \frac{M_k}{16\pi^2} \left\{ c_\alpha^2 \mathcal{F}\left(\frac{m_{H_1^0}^2}{M_k^2}\right) + s_\alpha^2 \mathcal{F}\left(\frac{m_{H_2^0}^2}{M_k^2}\right) - \mathcal{F}\left(\frac{m_{A^0}^2}{M_k^2}\right) \right\}. \quad (10)$$

In order to have an idea about the numerical values of different factors in (8), one writes

$$\frac{m^{(\nu)}}{0.05 \text{ eV}} \sim \left( \frac{h}{0.01} \right)^2 \left( \frac{M_k}{50 \text{ GeV}} \right) \left( \frac{\Lambda_k/M_k}{10^{-8}} \right). \quad (11)$$

The smallness of the parameters  $\Lambda_k$  in (10), and therefore of the neutrino mass, can be attained within two regimes: (1) the decoupling limit where the mixing  $|\sin \alpha| \ll 1$  is suppressed and the heavy  $CP$ -even mass is too large  $m_{H_2^0} \gg m_{A^0}$ ; and (2) the quasi-degenerate masses regime  $m_{H_2^0} \gtrsim m_{A^0} \gtrsim m_{H_1^0}$  while  $|\sin \alpha|$  can take any possible value between 0 and 1. Both the two regimes can be achieved with the two possible values of the heavy  $CP$ -even mass that can be extracted from (5), which are given by

$$m_{H_2^0} = m_{A^0} \frac{\sqrt{8 + t_{2\alpha}^2 \mp 4\sqrt{4 + t_{2\alpha}^2}}}{t_{2\alpha}}. \quad (12)$$

In the decoupling limit, the neutrino mass matrix elements (8) can be approximated to the minimal scotogenic model formula

$$im_{\alpha\beta}^{(v)} \simeq \frac{|\lambda_5|v^2}{16\pi^2} \sum_k \frac{h_{\alpha k} h_{\beta k} M_k}{\bar{m}^2 - M_k^2} \left[ 1 - \frac{M_k^2}{\bar{m}^2 - M_k^2} \log \frac{\bar{m}^2}{M_k^2} \right] \quad (13)$$

with  $\bar{m}^2 = (m_{H_1^0}^2 + m_{A^0}^2)/2$  and

$$\lambda_5 \simeq -\frac{s_\alpha^2 c_\alpha^2 (m_{H_1^0}^2 + m_{H_2^0}^2 - 2m_{A^0}^2)^2}{v^2 (m_{H_1^0}^2 + m_{H_2^0}^2 - m_{A^0}^2)}. \quad (14)$$

In the quasi-degenerate masses regime ( $m_{H_2^0} \gtrsim m_{A^0} \gtrsim m_{H_1^0}$ ), the effective coupling value is given by

$$\lambda_5 \simeq -\frac{m_{A^0}^2 - c_\alpha^2 m_{H_1^0}^2 - s_\alpha^2 m_{H_2^0}^2}{v^2}, \quad (15)$$

with  $\bar{m}^2 = (c_\alpha^2 m_{H_1^0}^2 + s_\alpha^2 m_{H_2^0}^2 + m_{A^0}^2)/2 \simeq m_{A^0}^2$ .

In the decoupling limit, by pushing the ratio  $m_{H_2^0}/m_{A^0}$  to larger values, the ratio  $\Lambda_k/M_k$  gets suppressed and therefore the neutrino mass smallness could be easily achieved. This scenario is much less tuned when compared with the minimal scotogenic model, where the neutrino mass smallness is guaranteed either via suppressed new Yukawa couplings  $h_{\alpha i}$ , or a suppressed value of the coupling  $\lambda_5 = O(10^{-9})$ . Moreover, the neutrino mass smallness could be achieved without decoupling  $H_2^0$  from the mass spectrum. In this case, all the three-neutral scalars are almost degenerate in mass  $m_{H_2^0} \simeq m_{H_1^0} \simeq m_{A^0}$  and the mixing angle is  $\alpha \simeq \pi/6$ . In this case, the equal  $CP$ -even contributions in (10) cancel the  $CP$ -odd one.

#### IV. THEORETICAL & EXPERIMENTAL CONSTRAINTS

In this section, we discuss the theoretical and the experimental constraints which we subject the model to. These constraints are briefly discussed below:

- **Perturbativity:** all the quartic couplings of the physical fields should be satisfy the perturbativity bounds, i.e.,

$$\lambda_{1,2,S}, |\omega_{1,2}|, |\lambda_3|, |\lambda_3 + \lambda_4| \leq 4\pi. \quad (16)$$

- **Perturbative unitarity:** the perturbative unitarity must be preserved in all processes involving scalars or gauge bosons. The scattering amplitudes, in the high-energy limit, contains four sub-matrices which decouple from each other due to the conservation of electric-charge,  $Z_2$  symmetry or  $CP$ -quantum numbers. We require that the eigenvalues of these matrices to be smaller than  $8\pi$ .

- **Vacuum Stability:** the scalar potential is required to be bounded from below in all the directions of the field space. Therefore, the following conditions need to be fulfilled:

$$\lambda_1, \lambda_2, \lambda_S, \lambda_1(\lambda_2\lambda_S - \bar{\omega}_2^2) - 9(\bar{\lambda}_3 + \bar{\lambda}_4)(\lambda_S(\bar{\lambda}_3 + \bar{\lambda}_4) - 3\bar{\omega}_1\bar{\omega}_2) + 9\bar{\omega}_1(3(\bar{\lambda}_3 + \bar{\lambda}_4)\bar{\omega}_2 - \lambda_2\bar{\omega}_1) > 0, \quad (17)$$

with  $\bar{X} = \min(X, 0)$ .

- **Gauge bosons decay widths:** The decay widths of the  $W/Z$ -bosons were measured with high precision at LEP. Therefore, we require that the decays of  $W/Z$ -bosons to  $Z_2$ -odd scalars is closed. This is fulfilled if one assumes that

$$m_{H_1^0} + m_{A^0} > M_Z, m_{H^\pm} + m_{A_1^0} > M_W, 2m_{H^\pm} > M_Z, m_{H^\pm} + m_{H_1^0} > M_W. \quad (18)$$

- **Lepton flavor violating (LFV) decays:** in this model, LFV decay processes arise via one-loop diagrams mediated by the  $H^\pm$  and  $N_k$  particles as in [30, 31]. We consider the decay branching ratios:  $\mathcal{B}(\ell_\alpha \rightarrow \ell_\beta + \gamma)$  and  $\mathcal{B}(\ell_\alpha \rightarrow \ell_\beta \ell_\beta \ell_\beta)$  whose analytical expressions can be found in e.g. [30], and require that are below the experimental upper bounds reported on by MEG and BABAR experiments [32, 33].
- **Direct searches of charginos and neutralinos at the LEP-II experiment:** we use the null results of neutralinos and charginos at LEP [34] to put lower bounds on the masses of charged Higgs  $H^\pm$  and the neutral scalars of the inert doublet. The bound obtained from a re-interpretation of neutralino searches [35] cannot apply to our model since the decays  $A^0 \rightarrow Z(\rightarrow \ell^+ \ell^-)H^\pm$  are kinematically forbidden. On the other hand, in most regions of the parameter space, the charged Higgs decays exclusively into a Majorana fermion and a charged lepton. For Yukawa couplings of order one  $h_{ei} \simeq \mathcal{O}(1)$ , the following bounds are derived  $m_{H^\pm} > 100$  GeV [16].
- **The electroweak precision tests:** in this model, the oblique parameters acquire contributions from the existence of inert scalars. We take  $\Delta U = 0$  in our analysis, the oblique parameters are given by [36]

$$\begin{aligned} \Delta T &= \frac{1}{16\pi s_W^2 M_W^2} \left\{ c_H^2 F(m_{H_1^0}^2, m_{H^\pm}^2) + s_H^2 F(m_{H_2^0}^2, m_{H^\pm}^2) + F(m_{A^0}^2, m_{H^\pm}^2) \right. \\ &\quad \left. - c_H^2 F(m_{H_1^0}^2, m_{A^0}^2) - s_H^2 F(m_{H_2^0}^2, m_{A^0}^2) \right\}, \\ \Delta S &= \frac{1}{24\pi} \left\{ (2s_W^2 - 1)^2 G(m_{H^\pm}^2, m_{H^\pm}^2, M_Z^2) + c_H^2 G(m_{H_1^0}^2, m_{A^0}^2, M_Z^2) \right. \\ &\quad \left. + s_H^2 G(m_{H_2^0}^2, m_{A^0}^2, M_Z^2) + c_H^2 \log \left( \frac{m_{H_1^0}^2}{m_{H^\pm}^2} \right) + s_H^2 \log \left( \frac{m_{H_2^0}^2}{m_{H^\pm}^2} \right) + \log \left( \frac{m_{A^0}^2}{m_{H^\pm}^2} \right) \right\}, \end{aligned} \quad (19)$$

where  $s_W \equiv \sin \theta_W$ , with  $\theta_W$  is the Weinberg mixing angle, and  $F(x, y)$  and  $G(x, y, z)$  are the one-loop functions which can be found in [36].

- **The signal strength  $\mu_h^{\gamma\gamma}$ :** the charged Higgs boson can change drastically the value of the Higgs boson loop-induced decay into two photons. The contribution of the charged Higgs boson depends on the sign of  $\lambda_3$ ; we obtain enhancement (suppression) of  $\Gamma(h \rightarrow \gamma\gamma)$  for negative (positive) values of  $\lambda_3$  [37]. We use the recent measurement of  $\mu_h^{\gamma\gamma} = \mathcal{B}(h \rightarrow \gamma\gamma)/\mathcal{B}(h \rightarrow \gamma\gamma)^{\text{SM}} = 1.02_{-0.12}^{+0.09}$  where we assume SM production rates for the SM Higgs boson [38].

## V. DARK MATTER

In this model, DM candidate could be either the light Majorana fermion ( $N_1$ ), the light  $CP$ -even scalar  $H_1^0$ , or a mixture of both components if they are degenerate in mass. In the case of scalar DM, the possible annihilation

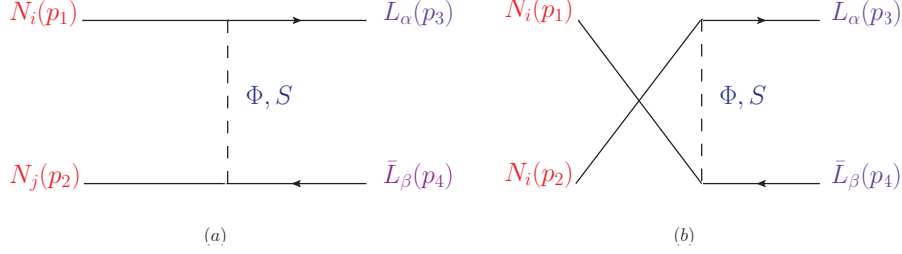


**FIG. 2:** DM (co-)annihilation diagrams, where  $L_\alpha$  denotes either charged lepton or neutrino, and  $\Phi, S$  denote  $H^\pm$  either or  $H_{1,2}^0, A^0$ .

channels are  $W^\pm W^\mp, ZZ, q_i \bar{q}_i, hh, \bar{\ell}_\alpha \ell_\beta$  and  $\bar{\nu}_\alpha \nu_\beta$ . In this scenario, however, the co-annihilation effect along the channel  $H_1^0 A^0 \rightarrow X_{SM} X'_{SM}$  is important due to the tiny mass difference  $(m_{A^0} - m_{H_1^0})/m_{A^0}$ . In this case, it is favored for the couplings  $h_{\alpha i}$  to be very small due to the LFV constraints, and therefore the contribution of the channels  $\nu_\alpha \bar{\nu}_\beta$  becomes negligible, which implies that this model with spin-0 DM is indistinguishable from the usual inert doublet model. In this case of Majorana fermion as a DM candidate, the DM self-(co-)annihilation could occur into charged leptons  $\ell_\alpha^- \ell_\beta^+$  (light neutrinos  $\nu_\alpha \bar{\nu}_\beta$ ) via  $t$ -channel diagrams mediated by the charged scalar  $H^\pm$  (the neutral scalars  $H_{1,2}^0, A^0$ ), as can be seen in Fig. 2.

The relic density is given by [39]

$$\frac{\Omega_{\text{DM}} h^2}{0.1198} \simeq \left(\frac{g_*}{100}\right)^{-1/2} \left(\frac{x_F}{25}\right) \left(\frac{\langle \sigma_{eff} v_r(x_F) \rangle}{1.830 \times 10^{-9} \text{ GeV}^{-2}}\right)^{-1}, \quad (20)$$

with  $g_*$  is the relativistic effective degrees of freedom that are in thermal equilibrium,  $x_F = M_1/T_F$  is the freeze-out parameter; and  $\langle \sigma_{eff} v_r(x_F) \rangle$  is the thermally averaged effective cross section at freeze-out, which is estimated by considering the co-annihilation effect [40] when it's important – see Appendix A for more details –. The inverse freeze-out temperature,  $x_F = M_1/T_F$ , can be determined iteratively by solving the transcendental equation [39]

$$x_F = \log \left( \frac{5}{4} \sqrt{\frac{45}{8}} \frac{M_1 M_{pl} \langle \sigma_{eff} v_r(x_F) \rangle}{\pi^3 \sqrt{g_* x_F}} \right). \quad (21)$$

Clearly, the relic density is inversely proportional to the combination  $\Theta = \sum_{\alpha\beta} |h_{\alpha 1} h_{\beta 1}^*|^2$ . In order to estimate the importance of the co-annihilation effect on the annihilation cross section, we show in Fig. 3-right, the ratio  $\Xi = \langle \sigma_{eff} v_r \rangle / (\zeta_{1,1} \langle \sigma(N_1 N_1) v_r \rangle)$ , where  $\langle \sigma_{eff} v_r \rangle$  is the full cross section within the co-annihilation effect (defined in Appendix A); and  $\zeta_{1,1} \langle \sigma(N_1 N_1) v_r \rangle$  is its  $N_1 N_1$  contribution. This ratio,  $\Xi$ , represents that the relative contribution to co-annihilation channels to the annihilation one. Note that  $\zeta_{1,1} = g_{eff}^{-2}$  is still depending on the freeze-out parameter  $x_F$ . In the right panel of Fig. 3, we display the allowed points in the model parameter space projected on the plan of the  $(H_1^0, H_2^0)$  masses. It can clearly be seen that there are two remarkable islands; one with quasi-degenerate scalars and another one with  $m_{H_2^0} \gg m_{H_1^0}$ .

## VI. COLLIDER SIGNATURES

In this section, we comment briefly on the collider implications of the model. The following discussion is based on two benchmark points which we display in Table II. In Fig. 4, we display the cross sections for the



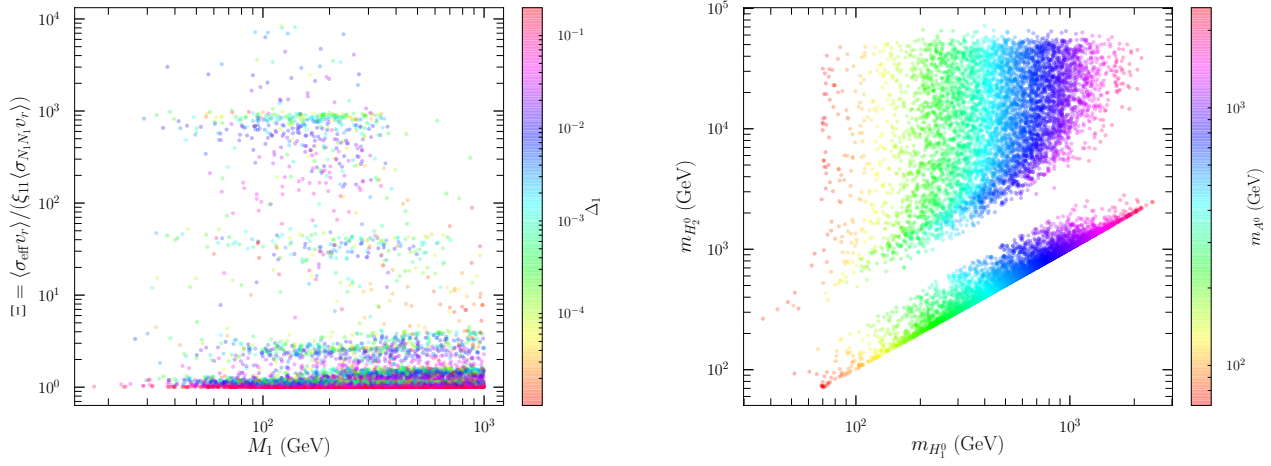


**FIG. 3:** *Left:* The ratio  $\Xi$  characterizing the strength of the co-annihilation cross section as a function of the DM mass  $M_1$  with the color bar showing the mass splitting  $\Delta_1 = (M_2 - M_1)/M_1$ . *Right:* Scatter plot on the plan of  $m_{H_1^0}$  and  $m_{H_2^0}$  with the palette showing  $m_{A^0}$ . The points shown in the two panels represent randomly chosen  $2 \times 10^4$  points that satisfy constraints from relic density, direct detection, theoretical constraints, and the electroweak precision tests.

pair production of the inert scalars as a function of the center-of-mass energy  $\sqrt{s}$  in hadronic collisions<sup>5</sup>. In the two benchmark scenarios, the  $H^\pm S$  production, with  $S = A^0, H_1^0$ , is dominant with a cross section of about 20 fb (100 fb) at  $\sqrt{s} = 14$  TeV which increases to around 400 fb (1 pb) at  $\sqrt{s} = 100$  TeV for BP1 (BP2). In the two benchmark scenarios,  $H_1^0$  and  $A^0$  decay invisibly into  $\nu_\ell N_k$  with 100% branching fraction. Moreover, the charged Higgs boson may decay into  $W^\pm H_1^0$  in the first benchmark scenario although with  $\mathcal{B} \simeq 21.1\%$ , and the remaining decays are into  $e^\pm N_k$  with branching fraction of 70.5% (100%) in BP1 (BP2). Therefore, the  $H^\pm S$  production leads exclusively to a  $e^\pm + E_T^{\text{miss}}$  signature which can be produced in the normal scotogenic model. The charged Higgs pair production occurs with a rate comparable to  $H^\pm H_1^0$ . On the other hand, this process will lead exclusively to a di-electron plus missing energy final state which also can occur in both the inert doublet and the scotogenic models. Besides, the pair production of neutral scalars  $A^0 H_1^0$ , and  $A^0 A^0$  leads to an invisible final state since both  $H_1^0$  and  $A^0$  decay invisibly. A possibility to make these processes visible at colliders is attaching an extra particle to the production channel such as a photon, jet or massive gauge boson. In this case, these processes cannot be considered smoking guns for the model as they occur in variety of scotogenic models with comparable rates.

The processes involving the heavy  $CP$ -even scalar ( $H_2^0$ ) can be extremely important in our scenarios. There are four production channels for  $H_2^0$ ;  $H_1^0 H_2^0$ ,  $A^0 H_2^0$ ,  $H^\pm H_2^0$  and  $H_2^0 H_2^0$ . The production rates of processes involving  $H_2^0$  are extremely small in the second scenario (see right panel of Fig. 4) with cross sections of order  $10^{-6}$ - $10^{-4}$  fb at the HL-LHC. Consequently, we concentrate our discussion on the first benchmark point for which the mass of  $H_2^0$  is about 349.64 GeV. First,  $H_2^0$  has four major decay channels;  $h H_1^0$ ,  $ZA^0$ ,  $\nu_\ell N_k$  and  $H^\pm W^\mp$  whose branching ratios are 58.7%, 21.56%, 11.5% and 7.6% respectively. The  $H^\pm H_2^0$  production channel occurs with the highest rate going from  $\simeq 1$  fb at 14 TeV to about 25 fb at 100 TeV. The signatures of this process can be split according to the decays of  $H_2^0$ , and the subsequent decays of the SM Higgs boson since  $H_1^0$

<sup>5</sup> The cross sections were computed with the help of MadGraph5\_aMC@NL0 version 2.7.0 [41] by using our UFO model file [42]. We used NNPDF30\_100as\_0118 with  $\alpha_s(M_Z) = 0.118$  [43] and renormalisation/factorisation scales  $\mu_{R,F} = 1/2 \sum_i (p_{T,i}^2 + m_i^2)$ .



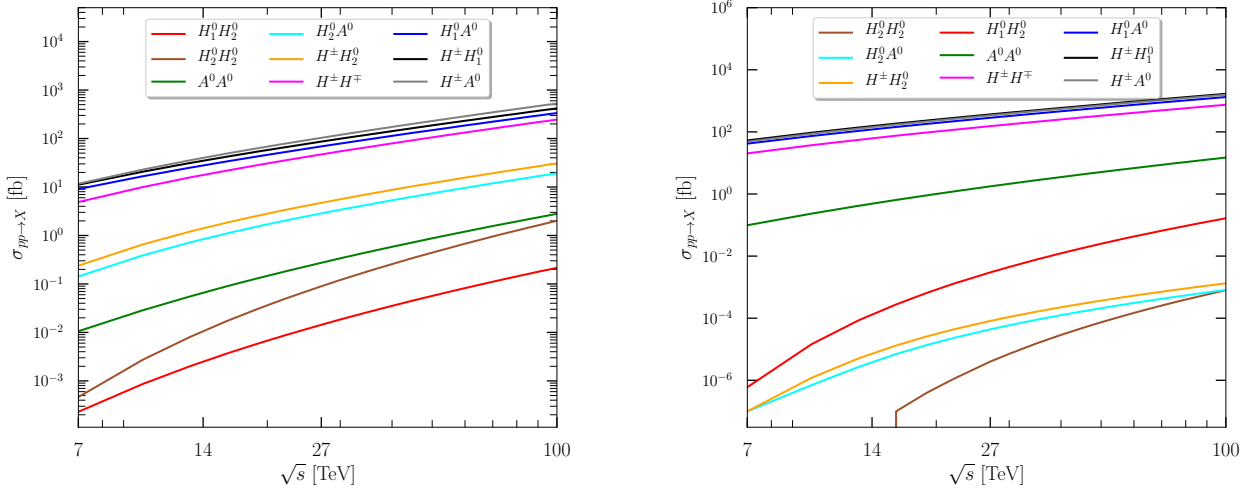


**FIG. 4:** The cross-section of pair production of inert scalars as a function of the center-of-mass energy  $\sqrt{s}$  in  $pp$ -collisions for BP1 (left) and BP2 (right). The results are shown for  $H_1^0 H_2^0$  (red),  $H_2^0 H_2^0$  (sienna),  $A^0 A^0$  (green),  $H_1^0 A^0$  (cyan),  $H^\pm H_2^0$  (orange),  $H^\pm H^\mp$  (rose),  $H_1^\pm A^0$  (blue),  $H^\pm H_1^0$  (black) and  $H^\pm A^0$  (gray).

decays invisibly with 100% branching ratio. In summary, we may have  $q\bar{q} + b\bar{b} + E_T^{\text{miss}}$ ,  $2e^\pm + 2\text{jets} + E_T^{\text{miss}}$ ,  $1e^\pm + 2\ell + E_T^{\text{miss}}$ ,  $1e^\pm + 2\text{jets} + E_T^{\text{miss}}$ , or  $1e^\pm + b\bar{b} + E_T^{\text{miss}}$ . On the other hand,  $A^0 H_2^0$  occurs with slightly smaller production cross section than that of  $H^\pm H_2^0$ . In this case, the  $CP$ -odd scalar  $A^0$  decays invisibly and the final states of this process consist of  $h/Z^0(\rightarrow b\bar{b}) + E_T^{\text{miss}}$ , or  $Z^0(\rightarrow \ell^+ \ell^-) + E_T^{\text{miss}}$  among others. Finally, the processes  $H_2^0 H_2^0$  and  $H_1^0 H_2^0$  have extremely small cross sections due to the fact they proceed through one-loop induced production with the exchange of the SM Higgs boson. In summary,  $H^\pm H_2^0$  and  $A^0 H_2^0$  are the only processes that have rich phenomenological implications at colliders and can be used to distinguish this model from the scotogenic model. We close this section by noting that a more detailed analysis of the collider implications of this model are postponed to a future study [44].

|     |   |  |  |
|-----|---|--|--|
| BP1 | $h_{\alpha i} = \begin{pmatrix} -0.73i & 0.068 + 0.021i & 0.057 + 0.069i \\ -8.86 \times 10^{-5} & -(105.27 + 0.64i) \times 10^{-6} & (6.60 - 0.539i) \times 10^{-6} \\ (6.60 + 9.72i) \times 10^{-6} & 6.07 \times 10^{-5} & 5.07 \times 10^{-5} \end{pmatrix}$                              |  |  |
|     | $m_{H_1^0} = 80.72 \text{ GeV}, m_{A^0} = 127.89 \text{ GeV}, m_{H_2^0} = 349.64 \text{ GeV}, m_{H^\pm} = 226.06 \text{ GeV}$   |  |  |
|     | $M_1 = 40.93 \text{ GeV}, M_2 = 46.37 \text{ GeV}, M_3 = 51.94 \text{ GeV}, \sin \alpha = 0.51$   |  |  |
| BP2 | $h_{\alpha i} = \begin{pmatrix} -0.85i & (8.05 + 2.49i) \times 10^{-2} & (6.73 + 8.13i) \times 10^{-2} \\ -5.91 \times 10^{-5} & (7.67 - 0.058i) \times 10^{-4} & -(9.10 + 0.046i) \times 10^{-4} \\ (5.05 + 7.44i) \times 10^{-5} & 4.65 \times 10^{-4} & 3.88 \times 10^{-4} \end{pmatrix}$ |  |  |
|     | $m_{H_1^0} = 120.25 \text{ GeV}, m_{A^0} = 126.59 \text{ GeV}, m_{H_2^0} = 2121.75 \text{ GeV}, m_{H^\pm} = 149.69 \text{ GeV}$   |  |  |
|     | $M_1 = 61.49 \text{ GeV}, M_2 = 61.86 \text{ GeV}, M_3 = 62.49 \text{ GeV}, \sin \alpha = 0.12$   |  |  |

**TABLE II:** Benchmark points

## VII. CONCLUSION

In this paper, we proposed a minimal extension of the so-called scotogenic model by a real singlet that mixes with the real part of the neutral inert component. In the minimal scotogenic model, when considering the lightest singlet Majorana fermion to be the dark matter candidate, the relic density requirements enforce

the Yukawa couplings  $h_{\alpha i}$  to be of the order  $\mathcal{O}(10^{-3} \sim 10^0)$  which requires a mass degeneracy between the  $CP$ -odd and  $CP$ -even neutral inert components ( $H^0$  and  $A^0$ ). This degeneracy implies a suppression in the quartic couplings  $\lambda_5$  in order to achieve the smallness of neutrino mass. In our extension, a global symmetry  $Z_4$ -symmetry forbids the  $\lambda_5$  term to exist; and the mixture of the real additional scalar with the real part of the inert component leads to two  $CP$ -even eigen states with the strict mass ordering  $m_{H_1^0} < m_{A^0} < m_{H_2^0}$ . In this setup, the neutrino mass smallness is achieved by the cancellation between three Feynmann diagrams instead of two in the minimal scotogenic. In consequence, we found two notable regimes on the mass spectrum of the model: the decoupling limit  $m_{H_1^0} \lesssim m_{A^0} \ll m_{H_2^0}$ ; and the quasi-degenerate one  $m_{H_1^0} \lesssim m_{A^0} \lesssim m_{H_2^0}$ .

We further studied the impact of various theoretical and experimental constraints on the model parameter space. We briefly discussed the collider phenomenology of the model by displaying the cross sections for two benchmark points corresponding to both the decoupling and the quasi-degenerate scenarios. We found that the quasi-degenerate scenarios are phenomenologically more interesting as they can lead to signatures which do not appear in the minimal scotogenic model, or in the inert doublet model. For instance, signatures with multi-jets and multi-leptons in addition to  $E_T^{\text{miss}}$  are the smokin-guns for these scenarios.

### Acknowledgments

The authors would like to thank L. Lavoura for his valuable remarks. The work of A. Jueid is supported by the National Research Foundation of Korea, Grant No. NRF-2019R1A2C1009419.

### Appendix A: The Annihilation Cross Section

The effective thermally averaged cross section at temperature  $T = M_1/z$  is given by [39]

$$\langle \sigma_{eff} v_r(z) \rangle = \frac{z}{8M_1^5 K_2^2(z)} \int_{4M_1^2}^{\infty} ds \langle \sigma_{eff}(s, z) v_r \rangle (s - 4M_1^2) \sqrt{s} K_1 \left( \frac{\sqrt{s}}{M_1} z \right), \quad (\text{A1})$$

is effective thermally averaged cross section at temperature  $T = M_1/z$ , with  $K_{1,2}$  are the modified Bessel functions.

Here,  $\langle \sigma_{eff} v_r(s, z) \rangle$  is the effective cross section where the co-annihilation effect is considered. Since only the Majorana fermions are considered to be quasi-degenerate, the effective cross section at CM energy  $\sqrt{s}$ , can be written as

$$\langle \sigma_{eff}(s, z) v_r \rangle = \sum_{i,j} \zeta_{i,j}(z) \langle \sigma_{ij}(s) v_r \rangle; \quad (\text{A2})$$

$$\zeta_{i,j}(z) = \frac{(1 + \Delta_i)^{3/2} (1 + \Delta_j)^{3/2} \exp\{-(\Delta_i + \Delta_j)z\}}{(\sum_k (1 + \Delta_k)^{3/2} \exp\{-\Delta_k z\})^2}, \quad (\text{A3})$$

with  $\Delta_k = (M_k - M_1)/M_1$ ; and  $\sigma_{ij} v_r$  is the cross section of the processes  $N_i N_j \rightarrow \ell^+ \ell^-, \nu \bar{\nu}$  at CM energy  $\sqrt{s}$ .

The relic density estimation (20) requires the cross section of each annihilation channel at the centre of mass energy  $\sqrt{s}$ . Here, the full amplitude of the process shown in Fig. 2 is given by

$$M = M_{(a)} - M_{(b)} = -i h_{\alpha i} h_{\beta j}^* \sum_X |\eta_X|^2 \left[ \frac{\bar{u}(p_3) P_L u(p_1) \bar{v}(p_2) P_R v(p_4)}{t - m_X^2} - \delta_{ij} (p_1 \longleftrightarrow p_2, t \longleftrightarrow u) \right], \quad (\text{A4})$$

where for  $\ell_\alpha^- \ell_\beta^+$  we have  $\eta_{H^\pm} = i$ , for  $\nu_\alpha \bar{\nu}_\beta$  we have  $\eta_{H_1^0} = i \frac{c_\alpha}{\sqrt{2}}$ ,  $\eta_{H_2^0} = i \frac{s_\alpha}{\sqrt{2}}$ ,  $\eta_{A^0} = \frac{1}{\sqrt{2}}$ ,  $t$  and  $u$  are the Mandelstam

variables; and  $P_{R,L} = (1 \pm \gamma^5)/2$ . The annihilation cross section  $\sigma_{ii}$  and  $\sigma_{ij}$  ( $j \neq i$ ) are given by [45]

$$\sigma_{ii} v_r = \frac{1}{32\pi s^2} \sum_{\alpha,\beta} \sum_{X,Y} \left| \eta_X \eta_Y h_{\alpha i} h_{\beta i}^* \right|^2 \lambda(s, m_\alpha^2, m_\beta^2) \{ \mathcal{R}(Q_X, Q_Y, T_+, T_-, B) + \\ - M_i^2 (s - m_\alpha^2 - m_\beta^2) \mathcal{K}(Q_X, Q_Y, B) \}, \quad (\text{A5})$$

$$\sigma_{ij} v_r = \frac{1}{64\pi s^2} \sum_{\alpha,\beta} \sum_{X,Y} \left| \eta_X \eta_Y h_{\alpha i} h_{\beta j}^* \right|^2 \lambda(s, m_\alpha^2, m_\beta^2) \mathcal{R}(Q_X, Q_Y, T_+, T_-, B), \quad (\text{A6})$$

with

$$\mathcal{R}(\alpha, \beta, \sigma, \theta, \eta) = \mathcal{R}(\alpha, \beta, \sigma, \theta, -\eta) = \int_{-1}^1 \frac{(\sigma + \eta t)(\theta + \eta t)}{(\alpha + \eta t)(\beta + \eta t)} dt, \quad \mathcal{K}(\alpha, \beta, \eta) = \int_{-1}^1 \frac{1}{(\alpha - \eta t)(\beta + \eta t)} dt. \quad (\text{A7})$$

$$\lambda(x, y, z) = \sqrt{(x - y - z)^2 - 4yz}, \quad B = \frac{1}{2s} \lambda(s, m_\alpha^2, m_\beta^2) \lambda(s, M_i^2, M_j^2) \\ Q_X = \frac{1}{2} (s + 2m_X^2 - M_i^2 - M_j^2 - m_\alpha^2 - m_\beta^2) + \frac{1}{2s} (M_i^2 - M_j^2)(m_\alpha^2 - m_\beta^2), \quad (\text{A8}) \\ T_\pm = \frac{1}{2} (s \pm M_i^2 \mp M_j^2 \pm m_\alpha^2 \mp m_\beta^2) + \frac{1}{2s} (M_i^2 - M_j^2)(m_\alpha^2 - m_\beta^2).$$

In (A5) and (A6), the summations should be performed over  $\{\alpha, \beta = \ell_\alpha^- \ell_\beta^+, X, Y = H^\pm\}$  and  $\{\alpha, \beta = \nu_\alpha \bar{\nu}_\beta, X, Y = A^0, H_{1,2}^0\}$ .

- 
- [1] A. Zee, *A Theory of Lepton Number Violation, Neutrino Majorana Mass, and Oscillation*, *Phys. Lett.* **93B** (1980) 389. [I](#)
  - [2] A. Zee, *Quantum Numbers of Majorana Neutrino Masses*, *Nucl. Phys.* **B264** (1986) 99.
  - [3] K. S. Babu, *Model of 'Calculable' Majorana Neutrino Masses*, *Phys. Lett.* **B203** (1988) 132.
  - [4] E. Ma, *Pathways to naturally small neutrino masses*, *Phys. Rev. Lett.* **81** (1998) 1171 [[hep-ph/9805219](#)].
  - [5] E. Ma, *Verifiable radiative seesaw mechanism of neutrino mass and dark matter*, *Phys. Rev.* **D73** (2006) 077301 [[hep-ph/0601225](#)]. [I](#)
  - [6] L. M. Krauss, S. Nasri and M. Trodden, *A Model for neutrino masses and dark matter*, *Phys. Rev.* **D67** (2003) 085002 [[hep-ph/0210389](#)].
  - [7] M. Aoki, S. Kanemura and O. Seto, *Neutrino mass, Dark Matter and Baryon Asymmetry via TeV-Scale Physics without Fine-Tuning*, *Phys. Rev. Lett.* **102** (2009) 051805 [[0807.0361](#)].
  - [8] M. Gustafsson, J. M. No and M. A. Rivera, *Predictive Model for Radiatively Induced Neutrino Masses and Mixings with Dark Matter*, *Phys. Rev. Lett.* **110** (2013) 211802 [[1212.4806](#)].
  - [9] T. Nomura and H. Okada, *A four-loop Radiative Seesaw Model*, *Phys. Lett. B* **770** (2017) 307 [[1601.04516](#)].
  - [10] T. Nomura, H. Okada and N. Okada, *A Colored KNT Neutrino Model*, *Phys. Lett. B* **762** (2016) 409 [[1608.02694](#)]. [I](#)
  - [11] Y. Cai, J. Herrero-García, M. A. Schmidt, A. Vicente and R. R. Volkas, *From the trees to the forest: a review of radiative neutrino mass models*, *Front.in Phys.* **5** (2017) 63 [[1706.08524](#)]. [I](#)
  - [12] S. M. Boucenna, S. Morisi and J. W. F. Valle, *The low-scale approach to neutrino masses*, *Adv. High Energy Phys.* **2014** (2014) 831598 [[1404.3751](#)]. [I](#)
  - [13] A. Ahriche, A. Jueid and S. Nasri, *Radiative neutrino mass and Majorana dark matter within an inert Higgs doublet model*, *Phys. Rev.* **D97** (2018) 095012 [[1710.03824](#)]. [1](#)
  - [14] T. Kitabayashi, *Scotogenic dark matter and single-zero textures of the neutrino mass matrix*, *Phys. Rev. D* **98** (2018) 083011 [[1808.01060](#)].
  - [15] D. Borah, P. B. Dev and A. Kumar, *TeV scale leptogenesis, inflaton dark matter and neutrino mass in a scotogenic model*, *Phys. Rev. D* **99** (2019) 055012 [[1810.03645](#)].
  - [16] A. Ahriche, A. Arhrib, A. Jueid, S. Nasri and A. de La Puente, *Mono-Higgs Signature in the Scotogenic Model with Majorana Dark Matter*, *Phys. Rev. D* **101** (2020) 035038 [[1811.00490](#)]. [IV](#)
  - [17] D. Mahanta and D. Borah, *Fermion dark matter with  $N_2$  leptogenesis in minimal scotogenic model*, *JCAP* **11** (2019) 021 [[1906.03577](#)].

- [18] T. Hugle, M. Platscher and K. Schmitz, *Low-Scale Leptogenesis in the Scotogenic Neutrino Mass Model*, *Phys. Rev. D* **98** (2018) 023020 [[1804.09660](#)].
- [19] A. Abada and T. Toma, *Electric Dipole Moments in the Minimal Scotogenic Model*, *JHEP* **04** (2018) 030 [[1802.00007](#)].
- [20] S. Baumholzer, V. Brdar, P. Schwaller and A. Segner, *Shining Light on the Scotogenic Model: Interplay of Colliders, Cosmology and Astrophysics*, [1912.08215](#).
- [21] D. Mahanta and D. Borah, *TeV Scale Leptogenesis with Dark Matter in Non-standard Cosmology*, *JCAP* **04** (2020) 032 [[1912.09726](#)].
- [22] P. Das, M. K. Das and N. Khan, *Dark matter, neutrino mass and baryogenesis in the radiative seesaw model*, [2001.04070](#).
- [23] D. Borah, A. Dasgupta, K. Fujikura, S. K. Kang and D. Mahanta, *Observable Gravitational Waves in Minimal Scotogenic Model*, [2003.02276](#). 1
- [24] R. Bouchand and A. Merle, *Running of Radiative Neutrino Masses: The Scotogenic Model*, *JHEP* **07** (2012) 084 [[1205.0008](#)]. I
- [25] L. Lopez Honorez, E. Nezri, J. F. Oliver and M. H. Tytgat, *The Inert Doublet Model: An Archetype for Dark Matter*, *JCAP* **02** (2007) 028 [[hep-ph/0612275](#)]. I
- [26] L. Sarma, P. Das and M. K. Das, *Scalar dark matter, leptogenesis and  $0\nu\beta\beta$  in minimal scotogenic model*, [2004.13762](#). I
- [27] A. Jueid and S. Nasri, *Searching for GeV-scale Majorana Dark Matter: inter spem et metum*, [2006.01348](#). I
- [28] A. Beniwal, J. Herrero-García, N. Leerdam, M. White and A. G. Williams, *The ScotoSinglet Model: A Scalar Singlet Extension of the Scotogenic Model*, [2010.05937](#). I
- [29] J. A. Casas and A. Ibarra, *Oscillating neutrinos and muon  $\rightarrow e, \gamma$* , *Nucl. Phys. B* **618** (2001) 171 [[hep-ph/0103065](#)]. III
- [30] T. Toma and A. Vicente, *Lepton Flavor Violation in the Scotogenic Model*, *JHEP* **01** (2014) 160 [[1312.2840](#)]. IV
- [31] M. Chekkal, A. Ahriche, A. B. Hammou and S. Nasri, *Right-handed neutrinos: dark matter, lepton flavor violation and leptonic collider searches*, *Phys. Rev. D* **95** (2017) 095025 [[1702.04399](#)]. IV
- [32] MEG collaboration, *New constraint on the existence of the  $\mu^+ \rightarrow e^+ \gamma$  decay*, *Phys. Rev. Lett.* **110** (2013) 201801 [[1303.0754](#)]. IV
- [33] BABAR collaboration, *Searches for Lepton Flavor Violation in the Decays  $\tau^+ \rightarrow e^+ \gamma$  and  $\tau^+ \rightarrow \mu^+ \gamma$* , *Phys. Rev. Lett.* **104** (2010) 021802 [[0908.2381](#)]. IV
- [34] DELPHI collaboration, *Searches for supersymmetric particles in  $e^+ e^-$  collisions up to 208-GeV and interpretation of the results within the MSSM*, *Eur. Phys. J. C* **31** (2003) 421 [[hep-ex/0311019](#)]. IV
- [35] E. Lundstrom, M. Gustafsson and J. Edsjo, *The Inert Doublet Model and LEP II Limits*, *Phys. Rev. D* **79** (2009) 035013 [[0810.3924](#)]. IV
- [36] W. Grimus, L. Lavoura, O. M. Ogreid and P. Osland, *The Oblique parameters in multi-Higgs-doublet models*, *Nucl. Phys. B* **801** (2008) 81 [[0802.4353](#)]. IV, IV
- [37] A. Arhrib, R. Benbrik, J. El Falaki and A. Jueid, *Radiative corrections to the Triple Higgs Coupling in the Inert Higgs Doublet Model*, *JHEP* **12** (2015) 007 [[1507.03630](#)]. IV
- [38] ATLAS collaboration, *Combined measurements of Higgs boson production and decay using up to  $80 \text{ fb}^{-1}$  of proton–proton collision data at  $\sqrt{s} = 13 \text{ TeV}$  collected with the ATLAS experiment*, . IV
- [39] M. Srednicki, R. Watkins and K. A. Olive, *Calculations of Relic Densities in the Early Universe*, *Nucl. Phys. B* **310** (1988) 693. V, V, A
- [40] J. Edsjo and P. Gondolo, *Neutralino relic density including coannihilations*, *Phys. Rev. D* **56** (1997) 1879 [[hep-ph/9704361](#)]. V
- [41] J. Alwall, R. Frederix, S. Frixione, V. Hirschi, F. Maltoni, O. Mattelaer et al., *The automated computation of tree-level and next-to-leading order differential cross sections, and their matching to parton shower simulations*, *JHEP* **07** (2014) 079 [[1405.0301](#)]. 5
- [42] C. Degrande, C. Duhr, B. Fuks, D. Grellscheid, O. Mattelaer and T. Reiter, *UFO - The Universal FeynRules Output*, *Comput. Phys. Commun.* **183** (2012) 1201 [[1108.2040](#)]. 5
- [43] NNPDF collaboration, *Parton distributions for the LHC Run II*, *JHEP* **04** (2015) 040 [[1410.8849](#)]. 5
- [44] A. Ahriche, A. Jueid and S. Nasri, *In progress*, . VI
- [45] I. Lalili, *The Annihilation Cross Section in Majorana Dark Matter Models: Exact Estimation*, Master thesis 2019, (Jijel, Algeria). A